

# Normalization of the Levi-Civita Hamiltonian at a collinear Lagrange point

Rocío I. Paez

Università degli Studi di Padova

Dipartimento di Matematica ‘Tullio Levi-Civita’

Via Trieste 63 - 35121 Padova, Italy

Massimiliano Guzzo

Università degli Studi di Padova

Dipartimento di Matematica ‘Tullio Levi-Civita’

Via Trieste 63 - 35121 Padova, Italy

June 25, 2022

## Abstract

The normalizations of the Hamiltonian of the circular restricted three-body problem at a collinear Lagrange equilibrium are used to compute approximations of its center and tube manifolds, as well as of all the dynamics in their neighbourhood. For small values of the reduced mass  $\mu$  the radius of convergence of any (even partial) normalization at  $L_1, L_2$  is affected by the complex singularities of the gravitational potential energy of the closest primary body, i.e. the one with smallest mass. In this paper we investigate if regularizations with respect to the body of mass  $\mu$  improve the convergence of the normalizations. In particular, we consider the Hamiltonian describing the planar three-body problem in Levi-Civita regularizing variables, and we show that for a suitable interval of the value of the Hamiltonian larger than the value at the Lagrange equilibrium, the Levi-Civita Hamiltonian has a fictitious center-saddle equilibrium at which the Hamiltonian can be normalized. We find that, for a sample value of  $\mu$  corresponding to the Sun-Jupiter mass ratio, the normalized regularized Hamiltonian provides approximation of the center and of the tube manifolds of  $L_1$  up to an energy corresponding to a Lyapunov orbit of amplitude which is larger than the distance  $|1 - \mu - x_{L_1}|$  of  $L_1$  from a complex singularity.

## 1 Introduction

The dynamics near the collinear Lagrange equilibria  $L_1, L_2$  of the circular restricted three-body problem has gained a lot of attention in the last decades because of its relevance for the study of the slow close encounters of a small body, for example a comet or a spacecraft, with a planet (see, for example, [4, 20, 19, 8, 9, 13, 14, 11, 21, 18, 12, 3]). Powerful methods to analyze these dynamics rely on the so called Hamiltonian reduction to the center manifold ([9, 13, 7]). Precisely, this is the explicit construction, for any value of an integer parameter  $N \geq 3$ , of a canonical transformation:

$$(x, y, z, p_x, p_y, p_z) = C_N(Q_1, Q_2, Q_3, P_1, P_2, P_3)$$

conjugating the Hamiltonian of the (spatial) circular restricted three-body problem :

$$h = \frac{p_x^2 + p_y^2 + p_z^2}{2} + p_x y - p_y x - \frac{\mu}{\sqrt{(x-1+\mu)^2 + y^2 + z^2}} - \frac{1-\mu}{\sqrt{(x+\mu)^2 + y^2 + z^2}} \quad (1)$$

to a normal form Hamiltonian<sup>1</sup>:

$$H = E_{L_i} + \sum_{j=2}^N K_j(Q_1, Q_2, Q_3, P_1, P_2, P_3) + \sum_{j \geq N+1} \mathcal{R}_j(Q_1, Q_2, Q_3, P_1, P_2, P_3), \quad (2)$$

which is analytic in some neighbourhood of the Lagrange equilibrium  $L_i$ , represented by  $(Q, P) = (0, 0)$  (the radius of the neighborhood depending on the mass ratio  $\mu$  and  $N$ ), and:

$$K_2 = \lambda Q_1 P_1 + \sum_{j=2}^3 \omega_j^2 \frac{P_j^2 + Q_j^2}{2}, \quad (3)$$

$K_j, \mathcal{R}_j$  are polynomials in the  $P, Q$  of order  $j$ , the polynomials  $K_j$  depend on the  $Q_1, P_1$  only through the product  $Q_1 P_1$  (alternative reduction methods can be considered, see Section 2 for details). We here refer to the usual units of masses, lengths and time for the three-body problem, so that the masses of the two massive bodies  $P_1$  and  $P_2$  are  $1 - \mu$  and  $\mu$  respectively, their coordinates in a barycentric Cartesian reference frame  $(x, y, z)$  are  $(-\mu, 0, 0)$  and  $(1 - \mu, 0, 0)$  and their revolution period is  $2\pi$ .

The canonical transformation  $C_N$ , obtained from a sequence of  $N$  Birkhoff normalizations (see Section 2), provides more than an approximation of the center manifold. In fact, by neglecting the remainder terms  $\mathcal{R}_j$  we obtain approximated equations of the level sets of the center manifold labelled by  $E \geq E_{L_i}$ :

$$\mathcal{M}_E = \left\{ Q, P : Q_1, P_1 = 0, \sum_{j=2}^3 \omega_j^2 \frac{P_j^2 + Q_j^2}{2} + \sum_{j=3}^N K_j(0, 0, Q_2, Q_3, P_2, P_3) = E \right\},$$

as well as for the (local) stable and unstable manifolds of  $\mathcal{M}_E$ :

$$W_E^s = \left\{ Q, P : Q_1 = 0, \sum_{j=2}^3 \omega_j^2 \frac{P_j^2 + Q_j^2}{2} + \sum_{j=3}^N K_j(0, Q_2, Q_3, P_1, P_2, P_3) = E \right\},$$

$$W_E^u = \left\{ Q, P : P_1 = 0, \sum_{j=2}^3 \omega_j^2 \frac{P_j^2 + Q_j^2}{2} + \sum_{j=3}^N \mathcal{K}_j(Q_1, Q_2, Q_3, 0, P_2, P_3) = E \right\}.$$

In the planar circular restricted three-body problem  $\mathcal{M}_E$  are curves supporting the so called horizontal Lyapunov orbits, and  $W_E^s, W_E^u$  are two-dimensional tubes.

Since  $E_{L_i}$  represents the value of the Hamiltonian  $h$  at the Lagrange equilibrium, for increasing values of  $E$ , in the set  $\mathcal{M}_E$  we find orbits of increasing libration amplitude (with respect to the equilibrium). As a consequence, for suitably large values of  $E$ , we expect a break down of the method. A natural limit for this break down is given by the singularity in the gravitational potential energy of the massive body  $P_2$  which, for small values of  $\mu$ , is close to  $L_1, L_2$ . We remark that, for the planar problem, the Lyapunov orbits  $\mathcal{M}_E$  are typically larger in the  $y$  coordinate with respect to the  $x$  coordinate, therefore a dangerous complex singularity is the one located at  $x = x_{L_j}$  and  $y = \pm i |1 - \mu - x_{L_j}|$  (for the Sun-Jupiter mass ratio, the singularity has  $y = \pm i 0.066\dots$ ), putting a severe limit to the validity of these methods for libration amplitudes in the  $y$  variable of order of  $|1 - \mu - x_{L_j}|$ . In this

<sup>1</sup>For convenience, we here consider in the Hamiltonian also the constant term  $E_{L_i}$  which is equal to the value of  $h$  computed at a Lagrange equilibrium  $L_i$ .

paper we investigate the possibility to overcome this limit by implementing the reduction to the center manifolds methods using the regularizations of the circular restricted three-body problem. Specifically, we consider the planar problem and the Levi-Civita transformation [17].

**Remarks:**

- (i) The motivations for this choice are twofold: on the one hand, the Levi-Civita transformation regularizing the planar problem is radically simpler than the Kustaanheimo-Stiefel ([15, 16] see also [1, 2]) transformation regularizing the spatial problem, and therefore it allows us to evidenciate sharply the advantages and the drawbacks of the reductions of a regularized Hamiltonian, rather than focusing on the geometric properties of the Kustaanheimo-Stiefel transformation. On the other hand, since in the planar problem the center manifold is made of periodic orbits, we have the possibility of a sharp comparison of the outcomes of the Hamiltonian reductions to the center manifold with the solution of the numerical integrations, since any small error in the determination of the initial condition is easily recognized as the distance on the numerically integrated orbit from a periodic one.
- (ii) Since in the planar problem the sets  $\mathcal{M}_E$  are curves supporting periodic orbits, one can find them also using general numerical methods designed for computing periodic orbits, such as the differential correction methods. The use of purely numerical methods to compute the horizontal Lyapunov orbits may work for libration amplitudes which are even much larger than the methods using Hamiltonian normalizations. However, the numerical methods do not provide an approximation of *all* the initial conditions in a neighbourhood of the periodic orbit, as the Hamiltonian normalizations do, and this is the fundamental information needed to study the slow transits of comets or spacecrafts close to a planet. For these reasons, we find it is interesting to investigate the validity of Hamiltonian normalizations as much as possible.

Following [17], we first perform the phase-space translation

$$X = x - x_{P_2}, \quad Y = y, \quad P_X = p_x, \quad P_Y = p_y - x_{P_2}, \quad (4)$$

where  $x_{P_2} = 1 - \mu$ , and then we introduce the Levi-Civita variables, extended to the momenta and to the fictitious time  $\tau$ ,

$$\begin{aligned} X &= u_1^2 - u_2^2, \quad Y = 2u_1u_2, \\ P_X &= \frac{U_1u_1 - U_2u_2}{2|u|^2}, \quad P_Y = \frac{U_1u_2 + U_2u_1}{2|u|^2}, \\ dt &= |u|^2 d\tau, \end{aligned} \quad (5)$$

where  $|u|^2 = u_1^2 + u_2^2$  while  $U = (U_1, U_2)$  denote the conjugate momenta to  $u = (u_1, u_2)$ . For any fixed value of  $E = E_{L_j} + E$  of the Hamiltonian (1) (restricted to the planar case  $z, p_z = 0$ ), the Levi-Civita Hamiltonian:

$$\begin{aligned} \mathcal{K}_E(u, U) &= \frac{1}{8} \left( U_1 + 2|u|^2 u_2 \right)^2 + \frac{1}{8} \left( U_2 - 2|u|^2 u_1 \right)^2 \\ &\quad - \frac{1}{2} |u|^6 - \mu - |u|^2 \left( E + \frac{(1-\mu)^2}{2} \right) - (1-\mu)|u|^2 \left[ \frac{1}{\sqrt{1 + 2(u_1^2 - u_2^2) + |u|^4}} + u_1^2 - u_2^2 \right], \end{aligned} \quad (6)$$

is a regularization of the planar three-body problem at  $P_2$ . In fact,  $\mathcal{K}_E$  is regular at  $u = (0, 0)$  (individuating a collision with  $P_2$ ), and the solutions  $(u(\tau), U(\tau))$  of the Hamilton equations of  $\mathcal{K}_E$  with initial conditions satisfying:  $u(0) \neq 0$  and  $\mathcal{K}_E(u(0), U(0)) = 0$ , are conjugate, for  $\tau$  in a neighbourhood of  $\tau = 0$ , via equations (5) to solutions  $(X(t), Y(t), P_X(t), P_Y(t))$  of the three-body problem Hamiltonian.<sup>2</sup>

From now on we focus our analysis for definiteness on the Lagrange equilibrium  $L_1$ ; the regularized Hamiltonian  $\mathcal{K}_E$  has, in particular, an equilibrium point at

$$(u_*, U_*) = (0, a(E), -2a(E)^3, 0) \quad (7)$$

for all the values of  $E$  in an interval  $E \in [E_{L_1}, E_*(\mu)]$ , which corresponds to the equilibrium  $L_1$  for  $E = E_{L_1}$ , and  $a(E)^2$  decreases monotonically with  $E$  up to  $a(E_*(\mu)) = 0$ . Except for  $E = E_{L_1}$ , we have  $\mathcal{K}_E(u_*, U_*) \neq 0$ , so that  $(u_*, U_*)$  does not correspond to a solution of the three-body problem, but nevertheless can be used to perform a Birkhoff normalization the Levi-Civita Hamiltonian (6). Then, from the normalized Hamiltonian, we define the center manifold  $\mathcal{M}_E$  as well as its stable and unstable manifold  $W_E^s, W_E^u$ . In this paper we describe all the steps necessary to perform the Birkhoff normalization of the Levi-Civita Hamiltonian, in particular we first show that the fictitious equilibria (7) are of center-saddle type. Then, we compare the numerical computation of Lyapunov orbits obtained from the normalization of the Levi-Civita Hamiltonian with the computations obtained from the normalizations using Cartesian variables. We find that, for the Sun-Jupiter mass ratio, the normalization of the Levi-Civita Hamiltonian provides Lyapunov orbits with amplitude which is larger than a factor  $1.4|1 - \mu - x_{L_1}|$ , and we discuss while for larger radii we observe a break-down of this method. We also compute the stable manifolds  $W_E^s$  for values of  $E$  such that the amplitude of the corresponding Lyapunov orbit is larger than  $|1 - \mu - x_{L_1}|$ . We remark that, to understand how the tube  $W_E^s$  folds around the singularity  $P_2$ , it is important to consider if the orbits with initial condition on the stable manifold very close to the Lyapunov orbit, when they are integrated backward in time, circulate around the singularity  $P_2$  clockwise or anticlockwise. We find that, while for small values of the energies, all such orbits perform the first circulation clockwise, for the largest values of the energy that we consider, we find that some of these orbits perform the first circulation clockwise while others perform the first circulation anticlockwise. As a consequence, in the two different cases, the projection of the tubes on the plane  $xy$  gives very different pictures.

## 2 Normalization of the Levi-Civita Hamiltonian at $L_1$

In this Section we describe the normalization of the Levi-Civita Hamiltonian providing the reduction to the center manifold. For definiteness, we describe the normalization at  $L_1$ .

**Equilibrium points of  $\mathcal{K}_E$ .** We first compute the fictitious equilibria of the Levi-Civita Hamiltonian, for different values of  $E$ , which are located at the  $x$ -axis and with  $x_1 < x < x_2$ , so that  $u_{*,1} = 0$ ,  $U_{*,2} = 0$ ,  $u_{*,2} = a \in (-1, 0)$ ,  $U_{1,*} = -2u_{2,*}^3$  where  $a$  satisfies  $F(a, E) = 0$  with

$$F(a, E) = -2 \left( E + \frac{1}{2}(1 - \mu)^2 \right) - 3a^4 + (1 - \mu) \left( 4a^2 - \frac{2a^2}{(1 - a^2)^2} - \frac{2}{1 - a^2} \right) \quad (8)$$

---

<sup>2</sup>The initial conditions of the regularized variables correspond to initial conditions of the original barycentric reference frame such that  $h(x(0), y(0), p_x(0), p_y(0)) = E$ .

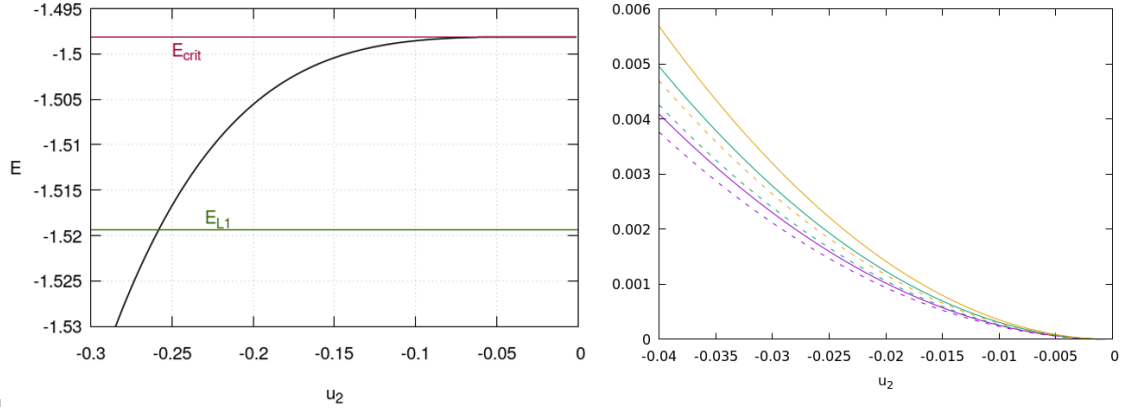


Figure 1: **Left panel:** The bold black line show the values of the energy  $E$  satisfying  $F(u_2, E) = 0$ , for  $u_2 \in [-0.3 : 0]$  and  $\mu = \mu_{Jup}$ . The green line labeled ' $E_{L_1}$ ' corresponds to the value of the energy of the Lagrangian point  $L_1$ . The purple line labeled ' $E_{crit}$ ' corresponds to the value of the critical energy  $E_*$ . **Right panel:** Representation of  $\lambda$  (continous lines) and  $\omega$  (dashed lines) for different values of  $\mu = 0, 0.25, 0.5$ .

The solutions  $(a, E)$  of the equation  $F(E, a) = 0$  are easily expressed in the form  $E = E(a)$ , represented in figure 1 for the Sun-Jupiter case. Note that:

- there exists a critical upper value for the energy,

$$E_* = -\frac{3}{2} \left( 1 - \frac{4}{3}\mu + \frac{1}{3}\mu^2 \right), \quad (9)$$

(e.g.  $E_* \sim -1.49809$  for  $\mu = \mu_{Jup} = 0.0009537$ ) for which the fictitious equilibrium is on the singularity at  $(u_1, u_2) = (0, 0)$ .

- since the sets  $\mathcal{M}_E$  exist only for  $E \geq 0$ , we have a natural lower limit for  $E > E_{L_1}$ .

Therefore,  $E$  is restricted to the interval  $E_{L_1} < E < E_*$ ; moreover, since

$$\frac{\partial F}{\partial a} > 0$$

for all  $\mu \in (0, 1/2)$  and  $a \in (-1, 0)$ , by denoting with  $a(E)$  the inverse function of  $E(a)$ , we have  $a \in (-a(E_{L_1}), 0)$ . In the following we continue the study by considering  $a \in (-a(E_{L_1}), 0)$  as a free parameter and determining  $E$  correspondingly.

**Remark:**

- (iii) The critical value (9) appears in the study of close encounters with  $P_2$  as a threshold value for considering a close encounters fast or slow (see, for example, section 3.1 of [10]). With this classification we are considering the regime of slow close encounters.
- (iv) For small values of  $\mu$ , the energy interval  $(E_{L_1}, E_*)$  seems small (i.e., for  $\mu = \mu_j$ , we have  $(E_{L_1}, E_*) \sim (-1.5193, -1.49809)$ ) but, as a matter of fact, tiny variations of the energy in this interval produce large variations in the amplitude of the Lyapunov orbits.

To determine the nature of the fictitious equilibria (7), we consider that the matrix representing the linearization of the Hamilton equations of  $\mathcal{K}_E$  at  $(u_*, U_*)$  (here written as a function of the parameter  $a$ , the energy being replaced by  $E(a)$ ):

$$M = \begin{pmatrix} 0 & \frac{3a^2}{2} & \frac{1}{4} & 0 \\ -\frac{a^2}{2} & 0 & 0 & \frac{1}{4} \\ \Gamma & 0 & 0 & \frac{a^2}{2} \\ 0 & -2\Gamma + a^4 & -\frac{3a^2}{2} & 0 \end{pmatrix}, \quad \Gamma = -a^4 + 4a^2(1 - \mu) \left(1 - \frac{1}{(1 - a^2)^3}\right) \quad (10)$$

has four eigenvalues  $\gamma$  which are the solutions of the quartic equation  $\det(M - \gamma \mathbb{I}) = 0$ , i.e.

$$\gamma = \pm \frac{1}{\sqrt{8}} \sqrt{-\Gamma - 5a^4 \pm \sqrt{9\Gamma^2 - 22a^4\Gamma - 15a^8}} := \pm \sqrt{\frac{A \pm \sqrt{B}}{8}}. \quad (11)$$

The nature of the eigenvalues is determined by the values of the functions  $A, B$ , which we compute numerically with reference to the domain of interest for  $a, \mu$ , which is identified as follows: for any  $\mu \in (0, 1/2)$ , we consider the interval  $a \in (a(E_{L_1}), 0)$ . We find that for all these values of  $a, \mu$  the fictitious equilibrium is of saddle-center type, with two imaginary eigenvalues  $\pm i\omega$  and two real eigenvalues  $\pm \lambda$ , with  $\lambda, \omega > 0$ . In particular, for  $a$  going to zero, both  $\lambda, \omega$  tend to zero as (a constant multiplying)  $a^2$  (see figure 1, left panel). The fact that for increasing  $E$ , the values of  $\lambda, \omega$  are decreasing, represents the main reason for the break down of the normalization method at suitably large  $E$ .

**The quadratic part of  $\mathcal{K}_E$  expanded at  $(u_*, U_*)$ .** For the values of  $E$  such that the Levi-Civita Hamiltonian  $\mathcal{K}_E$  has a saddle-center equilibrium in  $(u_*, U_*)$  there exists a canonical change of variables

$$(u, U) = A(q, p) + (u_*, U_*) \quad (12)$$

(note that  $q_2, p_2 \in \mathbb{C}$ , but for real values of  $u, U$  they satisfy  $q_2 = -ip_2$ ), conjugating  $\mathcal{K}_E(u, U)$  to the Hamiltonian

$$\mathcal{K}_E^{(0)}(q, p) = k_0 + k_2(q, p) + \sum_{j \geq 3} k_j(q, p), \quad (13)$$

where  $k_0 = \mathcal{K}_E(u_*, U_*)$ ,

$$k_2 = \lambda p_1 q_1 + i\omega q_2 p_2 \quad (14)$$

and  $k_j(q, p)$  are homogeneous polynomials of degree  $j$ . Hamiltonian in Eq. (13) is the starting point for the application of a Birkhoff normalizing algorithm. From now on, we will denote  $(q_1, q_2, p_1, p_2) = (\xi, q, \eta, p)$ , so that the couple of variables  $\xi, \eta$  is related to the hyperbolic behaviour, while the couple of variables  $q, p$  is related to the elliptic behaviour.

**Normalization of the Levi-Civita Hamiltonian at  $L_1$ .** We reproduce with the Levi-Civita Hamiltonian the methods of reduction to the center manifolds which have been introduced in the Cartesian variables ([13], [7]). Precisely, we perform a partial normal form scheme that uncouples (up to any arbitrary order) the hyperbolic variables  $\xi, \eta$  from the elliptic variables  $q, p$ . The reduction is done as usual with a near to the identity canonical transformation which conjugate the original Hamiltonian, expressed in terms of monomials of the type

$$\alpha_{k_1, l_1, k_2, l_2} q^{k_1} p^{l_1} \xi^{k_2} \eta^{l_2}, \quad (15)$$

to a transformed Hamiltonian with the following properties, according to different strategies:

- (a) the transformed Hamiltonian depends on the variables  $\xi, \eta$  only through their product  $\xi\eta$  (i.e. the canonical transformation eliminates every monomial for which  $k_2 \neq l_2$ , see [13]);
- (b) the transformed Hamiltonian contains two type of monomials (15): monomials independent of  $\xi, \eta$  and dependent on the  $q, p$  only through their product  $qp$ ; monomials at least quadratic in  $\xi, \eta$  (i.e. the canonical transformation eliminates every monomial for which  $k_2 + l_2 = 1$ , or those which simultaneously satisfy that  $k_2 + l_2 = 0$  and  $k_1 \neq l_1$ , see [7]);
- (c) the transformed Hamiltonian contains two type of monomials (15): monomials independent of  $\xi, \eta$ ; monomials at least quadratic in  $\xi, \eta$  (i.e. the canonical transformation eliminates every monomial for which  $k_2 + l_2 = 1$ ).

If one is interested only in the computation of the center manifold  $\mathcal{M}_E$  (the Lyapunov orbits for the planar case), then the best strategy is to adhere to the procedure that requires the minimum amount of eliminations, i.e. (b) or (c), so that one expects a largest radius of convergence of the normalized Hamiltonian (and a largest value of  $E$ ). If one is interested also in the computation of the stable and unstable manifolds  $W_E^s, W_E^u$ , and also of the dynamics in their neighbourhood, then one adheres to the procedure (a).

The reduction of order  $N$  is obtained by composition of  $N - 2$  sequence of near to the identity canonical transformations, called Birkhoff steps, conjugating the Hamiltonian  $\mathcal{K}_E^{(0)}(\xi, q, \eta, p)$  to the sequence:

$$\mathcal{K}_E^{(i)}(\xi, q, \eta, p) = k_0 + \sum_{j=2}^{i+2} K_j(\xi, q, \eta, p) + \sum_{j \geq i+3} \mathcal{R}_j^{(i)}(\xi, q, \eta, p), \quad i = 1, \dots, N-2 \quad (16)$$

where the  $K_j, \mathcal{R}_j^{(i)}$  are polynomials of order  $j$ , and the  $K_j$  are in normal form, according to the strategy (a),(b),(c) defined above,  $K_2 = k_2$  ( $k_0, k_2$  have been defined in (14)). For example, if we follow strategy (a), each canonical transformation of the sequence is the Hamiltonian flow at time 1 of the generating function  $\chi_i$  defined by

$$\chi_i = \sum_{k, l \in \mathbb{N}^2: \sum_n (k_n + l_n) = i+2, \quad k_2 \neq l_2} \frac{-\alpha_{k_1, l_1, k_2, l_2}^{(i-1)}}{i\omega(l_1 - k_1) + \lambda(l_2 - k_2)} q^{k_1} p^{l_1} \xi^{k_2} \eta^{l_2}, \quad (17)$$

where the coefficients  $\alpha_{k_1, l_1, k_2, l_2}^{(i)}$  are obtained from:

$$\mathcal{R}_j^{(i)} = \sum_{k, l \in \mathbb{N}^2: \sum_n (k_n + l_n) = j} \alpha_{k_1, l_1, k_2, l_2}^{(i)} q^{k_1} p^{l_1} \xi^{k_2} \eta^{l_2}. \quad (18)$$

We remark that the canonical transformations  $\mathcal{C}_{\chi_i}$  generated by  $\chi_i$ , the compositions of transformations  $\mathcal{C}_N = \mathcal{C}_{\chi_1} \circ \dots \circ \mathcal{C}_{\chi_{N-2}}$ , as well as the normalized Hamiltonian

$$\mathcal{K}_E^{(N)} = k_0 + \sum_{j=2}^N K_j(\xi, q, \eta, p) + \sum_{j \geq N+1} \mathcal{R}_j(\xi, q, \eta, p), \quad (19)$$

are explicitly constructed using the Lie series method (for an introduction to the method, see [6, 5] and references therein).

### 3 Numerical Examples

In this Section we describe how to use the normalization of the Levi-Civita Hamiltonian to compute the level sets  $\mathcal{M}_E$  of the center manifold as well as of their stable and unstable manifolds  $W_E^s$ ,  $W_E^u$ , and we provide some comparisons with the normalizations implemented using the Cartesian variables.

For a given value of  $a \in (a(E_{L_1}), 0)$ , corresponding to an energy  $E$ , one first computes the normalized Levi-Civita Hamiltonian (19) (according to the strategies (a), (b) or (c)) for a certain order  $N$  of normalization, so that the remainder terms  $\mathcal{R}_j$  are polynomials of degree larger than  $N$ . Then, we neglect the remainder terms  $\mathcal{R}_j$  in the normalized Hamiltonian and we remain with

$$\hat{\mathcal{K}}_E^{(N)} = k_0 + \sum_{j=2}^N K_j(\xi, q, \eta, p).$$

Independently on the strategy (a),(b),(c), the set  $\mathcal{M}_E$  is represented in the normalized variables by

$$\mathcal{M}_E = \left\{ \xi, q, \eta, p : \quad \xi, \eta = 0, \quad k_0 + \sum_{j=2}^N K_j(0, q, 0, p) = 0 \right\},$$

and then it is mapped back to the original variables using the inverse of the canonical transformation  $\mathcal{C}_N$  and all the transformations needed to pass from the Cartesian variables  $(x, y, p_x, p_y)$  to the regularized variables  $(u, U)$  and to the variables  $(\xi, q, \eta, p)$ .

**Remark:**

- (v) The error in computing the set  $\mathcal{M}_E$  by neglecting the remainder terms  $\mathcal{R}_j$  depends on the norm of the remainder in the set  $\mathcal{M}_E$ , which is bounded by

$$\left\| \sum_{j \geq N+1} \mathcal{R}_j(\xi, q, \eta, p) \right\| \leq \alpha_N \rho^N$$

where the coefficient  $\alpha_N$  depends on  $N$  and where  $\rho$  denotes the maximum amplitude in the variables  $q, p$  of the set  $\mathcal{M}_E$ . In principle, one wishes to use the largest possible value of  $N$  which is compatible with a reasonable CPU time and memory usage of modern computers. However, as it is typical of normalizing transformations, the coefficients  $\alpha_N$  can increase with  $N$  so that it may happen that  $\alpha_N \rho^N$  decreases only up to a certain value of  $N$ , depending on  $\rho$ . In this paper, we do not quantify a priori these errors, but we will set up a numerical method to estimate their effects. In particular, rather than constructing the stable and unstable sets  $W_E^s, W_E^u$ , we will construct two surfaces, which we call the inner and outer stable/unstable tubes, containing the sets  $W_E^s, W_E^u$ .

- (vi) The values of the coefficients  $\alpha_N$  increase also as the energy  $E$  increases, since the values of  $\lambda, \omega$ , which appear at the denominators of the generating functions  $\chi_i$ , decrease. Moreover, since also  $\rho$  increases as the energy increases, we have an increment of the error terms  $\alpha_N \rho^N$  which limits the validity of the method up to a certain value of  $a_c \in (a(E_{L_1}), 0)$ .



The stable and unstable manifolds  $W_E^s, W_E^u$  are instead computed from the normalization implemented using strategy (a). In this case, the sets are represented in the normalized variables by

$$W_E^s = \left\{ \xi, q, \eta, p : \xi = 0, \quad k_0 + \sum_{j=2}^N K_j(0, q, \eta, p) = 0 \right\},$$

$$W_E^u = \left\{ \xi, q, \eta, p : \eta = 0, \quad k_0 + \sum_{j=2}^N K_j(\xi, q, 0, p) = 0 \right\},$$

and then mapped back to the original Cartesian variables  $(x, y, p_x, p_y)$ . As a matter of fact, since the normalizing transformation is valid only in a small neighbourhood of the set  $\mathcal{M}_E$ , we compute the following sections of the stable and unstable manifolds:

$$\begin{aligned} \left\{ \xi, q, \eta, p : \xi = 0, \eta = \eta_0, \quad k_0 + \sum_{j=2}^N K_j(0, q, \eta_0, p) = 0 \right\} &\subseteq W_E^s, \\ \left\{ \xi, q, \eta, p : \xi = \xi_0, \eta = 0, \quad k_0 + \sum_{j=2}^N K_j(\xi_0, q, 0, p) = 0 \right\} &\subseteq W_E^u, \end{aligned} \quad (20)$$

with suitably small values of  $\eta_0 \neq 0, \xi_0 \neq 0$ . Then, the tubes  $W_E^s, W_E^u$  are constructed by computing numerically the orbits with initial conditions in a grid of points of (20).

We quantify the effect of the errors in the computation of the sets  $\mathcal{M}_E, W_E^s, W_E^u$  as follows:

- (1) We consider a point in the set  $\mathcal{M}_E$ , computed as explained above. Then, we represent it in the Levi-Civita variables  $(u, U)$ , we integrate numerically the Hamilton equations of the Levi-Civita Hamiltonian (6) and we represent the solution in the Cartesian variables  $(x(t), y(t))$ . In the case the initial condition is on the Lyapunov orbit, without any error, the numerical integration should provide a periodic orbit of period  $T$ ; otherwise, the numerically integrated orbit does not exactly closes after  $T$ , and the distance of  $(x(T), y(T))$  from  $(x(0), y(0))$  provides an estimate of the error in the computation of  $\mathcal{M}_E$ .
- (2) We consider for definiteness the stable manifold, and its branch which extends on the right of the Lyapunov orbit, towards the singularity; the set  $W_E^s$  computed from the first of equations (20) is affected by some error. But, as done in [12], we can profit of a property of the tube manifolds to construct numerically two surfaces, which we call the inner and outer stable tubes  $W_E^{s,in}, W_E^{s,out}$ , that contain the true stable manifold  $W_E^s$ . As soon as the two surfaces  $W_E^{s,in}, W_E^{s,out}$  are very close, the numerical errors in the computation of  $W_E^s$  is small.

The inner and outer stable tubes are defined as by computing the two cycles:

$$\begin{aligned} \left\{ \xi, q, \eta, p : \xi = \xi_0, \eta = \eta_0, \quad k_0 + \sum_{j=2}^N K_j(\xi_0, q, \eta_0, p) = 0 \right\} \\ \left\{ \xi, q, \eta, p : \xi = -\xi_0, \eta = \eta_0, \quad k_0 + \sum_{j=2}^N K_j(-\xi_0, q, \eta_0, p) = 0 \right\} \end{aligned} \quad (21)$$

with  $0 < \xi_0 < \eta_0$ . The parameters  $\xi_0, \eta_0$  are chosen so that by computing the initial condition on the two cycles (21) forward in time, we observe that all the orbits with initial conditions on one cycle approach the Lyapunov orbit and then bounce back on the right, while all the orbits with initial conditions on the other cycle approach the Lyapunov orbit and then transit on the left. Since the stable manifold is a separatrix for the motions which approach the Lyapunov orbit and then transit on the left or

bounce back to the right, by computing the backward evolution of orbits with initial conditions in the cycles (21) we obtain two tubes containing the tube manifold  $W_E^s$ .

We here report some computations for the Lagrangian equilibrium  $L_1$ , using the Sun-Jupiter mass ratio. In figure 2 we represent the Lyapunov orbits computed using method (a) (right panel), and method (c), left panel. As it was expected, with the method (c) we reach a larger value for the amplitude of the Lyapunov orbit with respect to the method (a). In figure 3 we show for comparison the computation of Lyapunov orbits using the normalization of the Hamiltonian expressed with the Cartesian variables. We observe that the largest Lyapunov orbit obtained with the Cartesian variables-strategy (b) is comparable with the largest Lyapunov orbit obtained with the Levi-Civita variables-strategy (c), even if the amplitude is well beyond the limit of the complex singularity in the gravitational potential generated by  $P_2$ . A possible explanation is that the difference between the potential energy and its Taylor expansion at  $L_1$ , for these values of the libration, is mitigated by the multiplying factor  $\mu \sim 10^{-3}$ . Instead, the largest Lyapunov orbit obtained with the Cartesian variables-strategy (a) corresponds approximately to the distance  $|1 - \mu - x_{L_1}|$  of a complex singularity from  $L_1$ . A possible explanation of the fact that the method (a) does not work beyond the complex singularity could be in the largest number of terms to eliminate to put the Hamiltonian in normal form. Since for the computation of the stable and unstable manifolds we are forced to use method (a), we have an indication of the improvement introduced by the Levi-Civita variables, which allowed us to reach a libration amplitude of about  $1.4 |1 - \mu - x_{L_1}|$ .

In figures 4, 5, 6, we represents the inner and outer stable tubes computed using the normalized Levi-Civita Hamiltonian, for  $a = 0.255, 0.25, 0.23$ . From the top panels we appreciate that the inner and outer stable manifolds are correctly identified; from the right panels we appreciate the computation of longer parts of the inner and outer tube. It is remarkable that for the smaller values of  $a$  ( $a = 0.255, 0.25$ ), all the orbits on both tubes departing from the sets (21) backward in time transit at the right of the body  $P_2$ , while for  $a = 0.23$  (see figures 6 and 7) there are orbits that transit on the right and also orbits that transit on the left of  $P_2$ . As a consequence, in the two different cases, the projection of the tubes on the plane  $xy$  gives very different pictures.

**Acknowledgments.** R.P. is supported by the ERC project 677793 StableChaoticPlanetM and this research is part of this project. MG and RP wish to thank Gabriella Pinzari for useful discussions.

## References

- [1] F. Cardin and M. Guzzo: "Integrability of the spatial three-body problem near collisions (an announcement)". In press on Rendiconti Lincei, Matematica e Applicazioni, 2019.
- [2] F. Cardin, M. Guzzo, "Integrability of the spatial restricted three-body problem near collisions", *arXiv:1809-01257* (2018).
- [3] Celletti A., Pucacco G., Stella D., "Lissajous and Halo orbits in the restricted three-body problem", *J. Nonlinear Science*, vol. 25, Issue 2, 343-370 (2015).
- [4] Conley C., Easton R., Isolated invariant sets and isolating blocks, *Transactions of the American Mathematical Society* 158, 35-61, 1971.

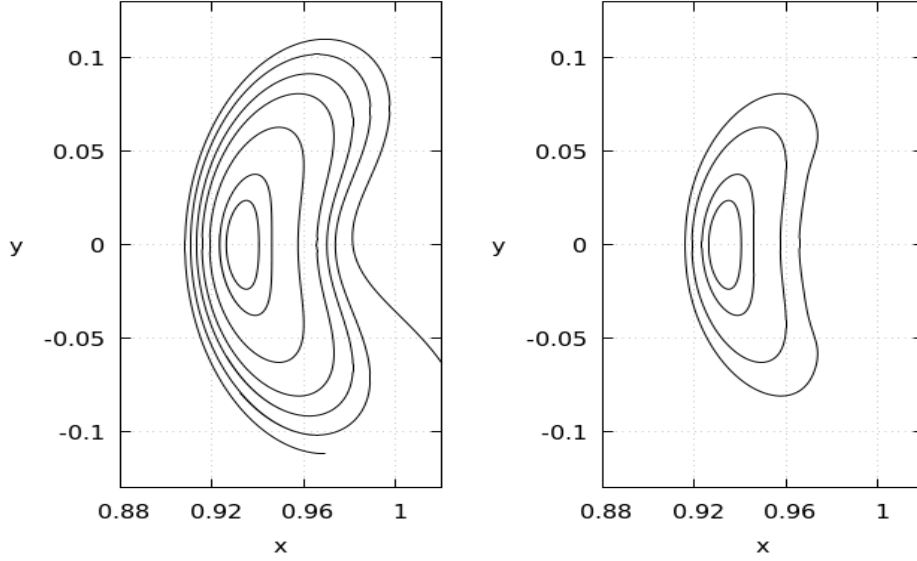


Figure 2: Lyapunov orbits of different amplitudes computed by normalizing the Levi-Civita Hamiltonian with the method (a) (right panel) and method (c) (left panel). The initial conditions have been obtained from the normalized Levi-Civita Hamiltonian, while the orbits have been numerically computed by integrating the non-normalized Hamiltonian  $\mathcal{K}_E$ . Therefore, the error in the computation of the initial condition introduced by neglecting the remainder of the normal form determines that the orbits do not close exactly after the period of the Lyapunov orbit. For large amplitudes it happens (like the open orbit in the right panel) that the error does not improve by increasing the order of the normalization.

- [5] C. Efthymiopoulos, “Canonical perturbation theory, stability and diffusion in Hamiltonian systems: applications in dynamical astronomy”, *Cincotta, P., Giordano, C., & Efthymiopoulos, C. (eds.), Proceedings of the Third La Plata School on Astronomy and Geophysics, AAS 3* (2011)
- [6] Giorgilli, A., “Notes on exponential stability of Hamiltonian systems”, in *Dynamical Systems. Part I: Hamiltonian Systems and Celestial Mechanics*, Pubblicazioni della Classe di Scienze, Scuola Normale Superiore, Pisa, 2002.
- [7] A. Giorgilli, “On a theorem of Lyapounov”, *Rendiconti dell’Istituto Lombardo Accademia di Scienze e Lettere, Classe di Scienze Matematiche e Naturali*, 146, 133 (2012)
- [8] Gomez G., Koon W.S., Lo M.W., Marsden J.E., Masdemont J. and Ross S.D., Connecting orbits and invariant manifolds in the spatial restricted three-body problem, *Nonlinearity*, 17, 1571-1606, 2004.
- [9] Gómez G., Jorba À., Masdemont J., Simó C., *Dynamics and Mission Design Near Libration Point Orbits, Vol. 3: Advanced Methods for Collinear Points*, World Scientific, Singapore, 2000.
- [10] Guzzo M., Lega E., On the identification of multiple close encounters in the planar circular restricted three-body problem, *MNRAS*, vol. 428, pag. 2688-2694, 2013.

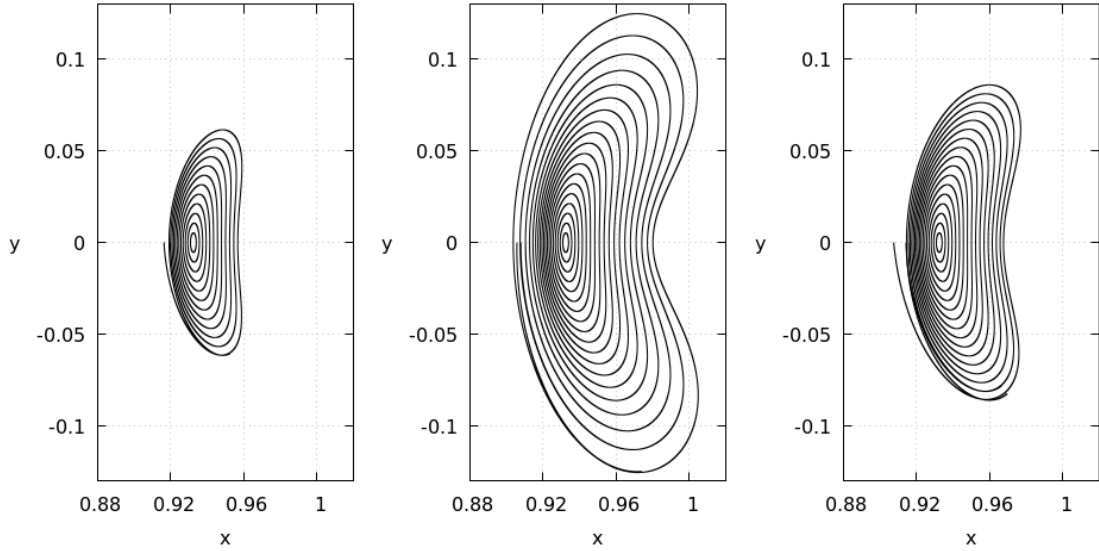


Figure 3: Lyapunov orbits of different amplitudes computed by normalizing the Hamiltonian in the Cartesian variables with the method (a) (left panel), method (b) (center panel) and method (c) (right panel). The initial conditions have been obtained from the normalized Cartesian Hamiltonian, while the orbits have been numerically computed by integrating the non-normalized regularized Hamiltonian  $\mathcal{K}_E$ . Therefore, the error in the computation of the initial condition introduced by neglecting the remainder of the normal form determines that the orbits do not close exactly after the period of the Lyapunov orbit. For large amplitudes it happens (like the open orbits in all the panels) that the error does not improve by increasing the order of the normalization.

- [11] Guzzo M., Lega E., Evolution of the tangent vectors and localization of the stable and unstable manifolds of hyperbolic orbits by Fast Laypunov Indicators, SIAM J. APPL. MATH., Vol. 74, No. 4, pp. 1058-1086, 2014.
- [12] Guzzo M. and Lega E.: "Geometric chaos indicators and computations of the spherical hypertube manifolds of the spatial circular restricted three-body problem", Physica D, vol. 373, 35-58, 2018.
- [13] A. Jorba. J. Masdemont, "Dynamics in the center manifold of the collinear points of the restricted three body problem", *Phisica D*, **132**, 189 (1999)
- [14] Koon W.S., Lo M.W., Marsden J.E. and Ross S.D., Dynamical Systems, the three body problem and space mission design. Marsden Books. ISBN 978-0-615-24095-4, 2008.
- [15] Kustaanheimo P., Spinor regularisation of the Kepler motion, Annales Universitatis Turkuensis A 73, 1-7. Also Publications of the Astronomical Observatory Helsinki 102, 1964.
- [16] Kustaanheimo P. and Stiefel E.L., Perturbation theory of Kepler motion based on spinor regularization, Journal fur die Reine und Angewandte Mathematik 218, 204-219, 1965.
- [17] T. Levi-Civita, "Sur la régularisation qualitative du problème restreint des trois corps", *Acta Math.*, **30**, 305 (1906).

- [18] Lega E. and Guzzo M.: "Three-dimensional representations of the tube manifolds of the planar restricted three-body problem", *Physica D*, 352:41-52, 2016.
- [19] Masdemont J.J., High Order Expansions of Invariant Manifolds of Libration Point Orbits with Applications to Mission Design, *Dynamical Systems: An International Journal*, vol. 20, no. 1, pp. 59-113, 2005.
- [20] Simó C., Dynamical systems methods for space missions on a vicinity of collinear libration points, in Simó, C., editor, *Hamiltonian Systems with Three or More Degrees of Freedom* (S'Agaró, 1995), volume 533 of *NATO Adv. Sci. Inst. Ser. C Math. Phys. Sci.*, pp. 223-241, Dordrecht. Kluwer Acad. Publ., 1999.
- [21] Zanzottera A., Castelli R., Mingotti G., and Dellnitz M., Intersecting invariant manifolds in spatial restricted three-body problems: Design and optimization of Earth-to-halo transfers in the Sun-Earth-Moon scenario, *Communications in Nonlinear Science and Numerical Simulation*, vol. 17, no. 2, pp. 832-843, 2012.

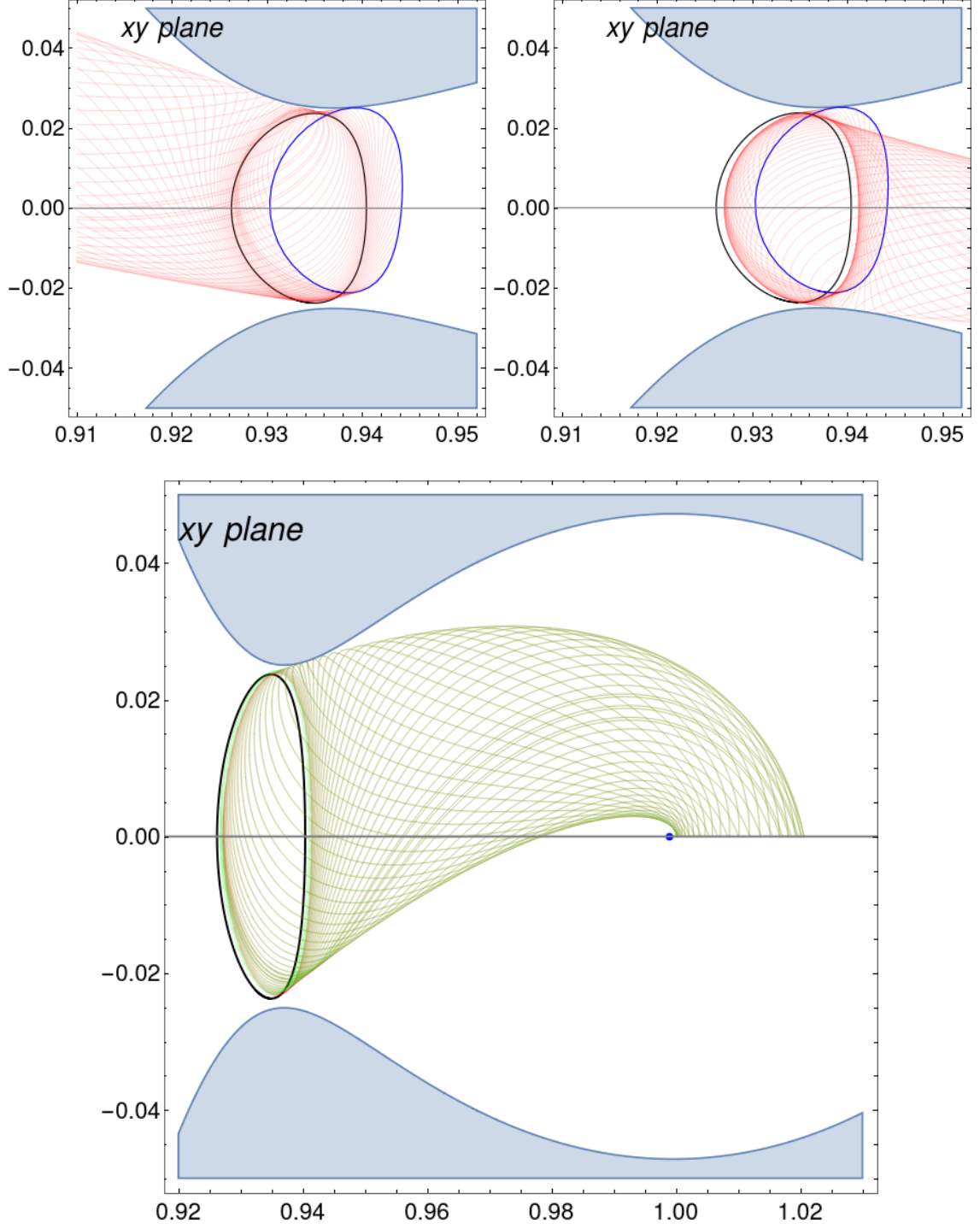


Figure 4: Representation of the inner and outer stable tubes for  $a = -0.255$ . On the top panels we represent separately the orbits with initial conditions of both tubes integrated forward in time approaching in both cases the Lyapunov orbit, but then the orbits on one tube bounce back, while the orbits on the other tube transit on the left of the Lyapunov orbit. On the bottom panel we represent the orbits with initial conditions of both tubes (in green and red respectively) integrated backward in time. We appreciate that they are almost overlapped. The black curve represents the Lyapunov orbit, the blue curves represent initial conditions in the inner and outer tubes, the shaded area represents the realm of forbidden motions for this value of the energy.

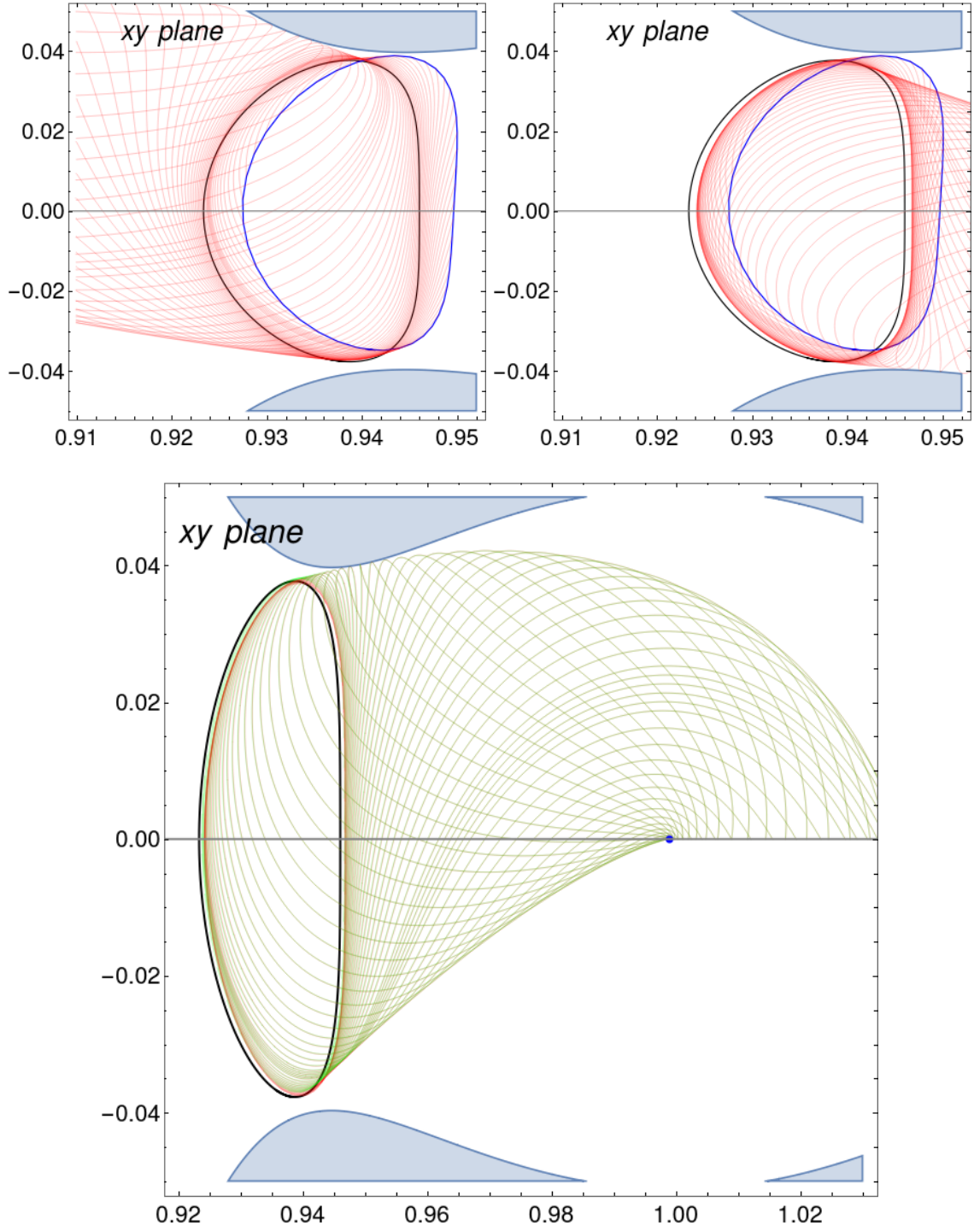


Figure 5: Same as figure 4 for  $a = -0.25$ . We remark that the secondary body  $P_2$  is very close, but still locate outside both tubes (see the zoomed in, left panel, of figure 7).

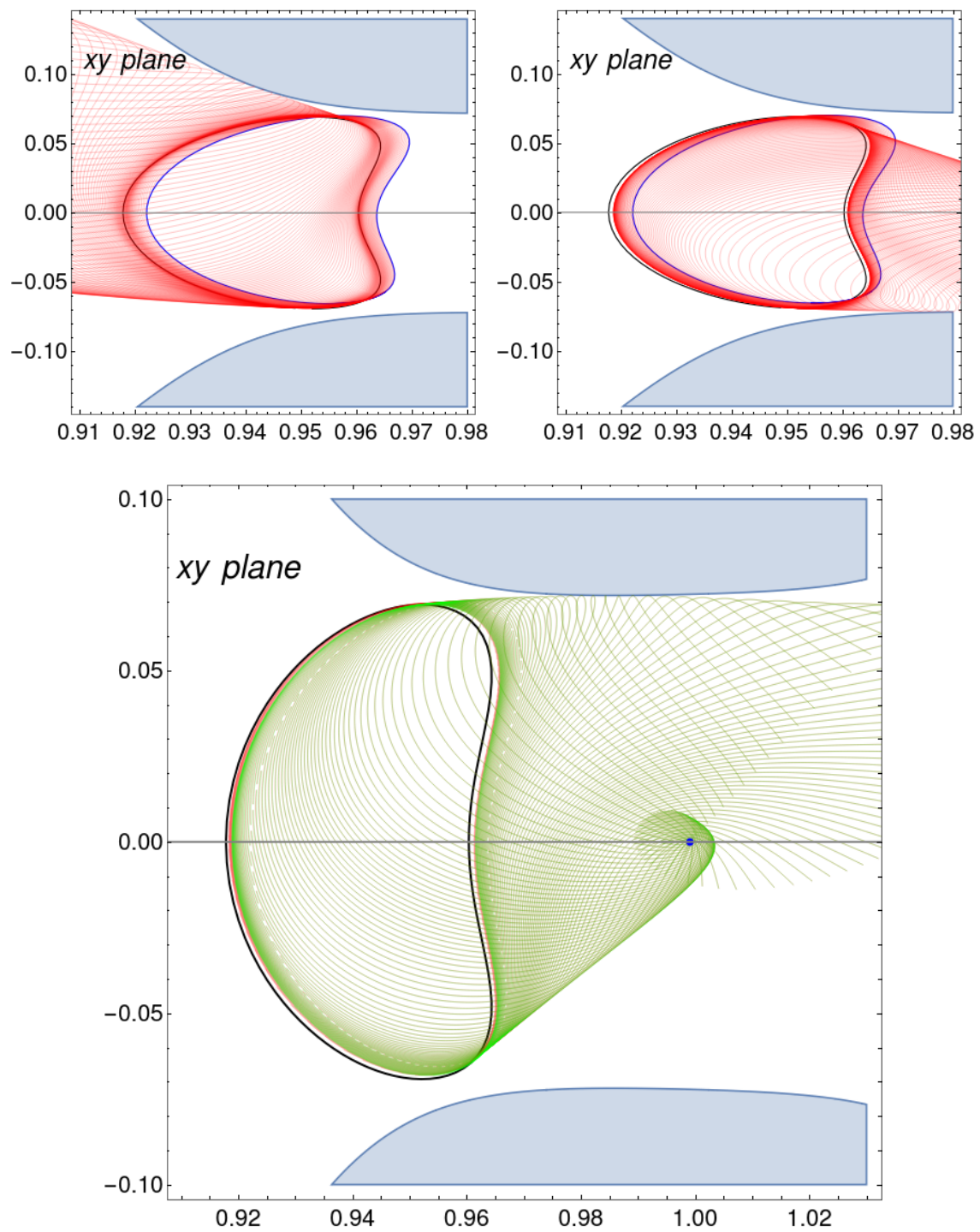


Figure 6: Same as figure 4 for  $a = -0.23$ . To better appreciate how the tubes circulate around  $P_2$ , see figure 7.



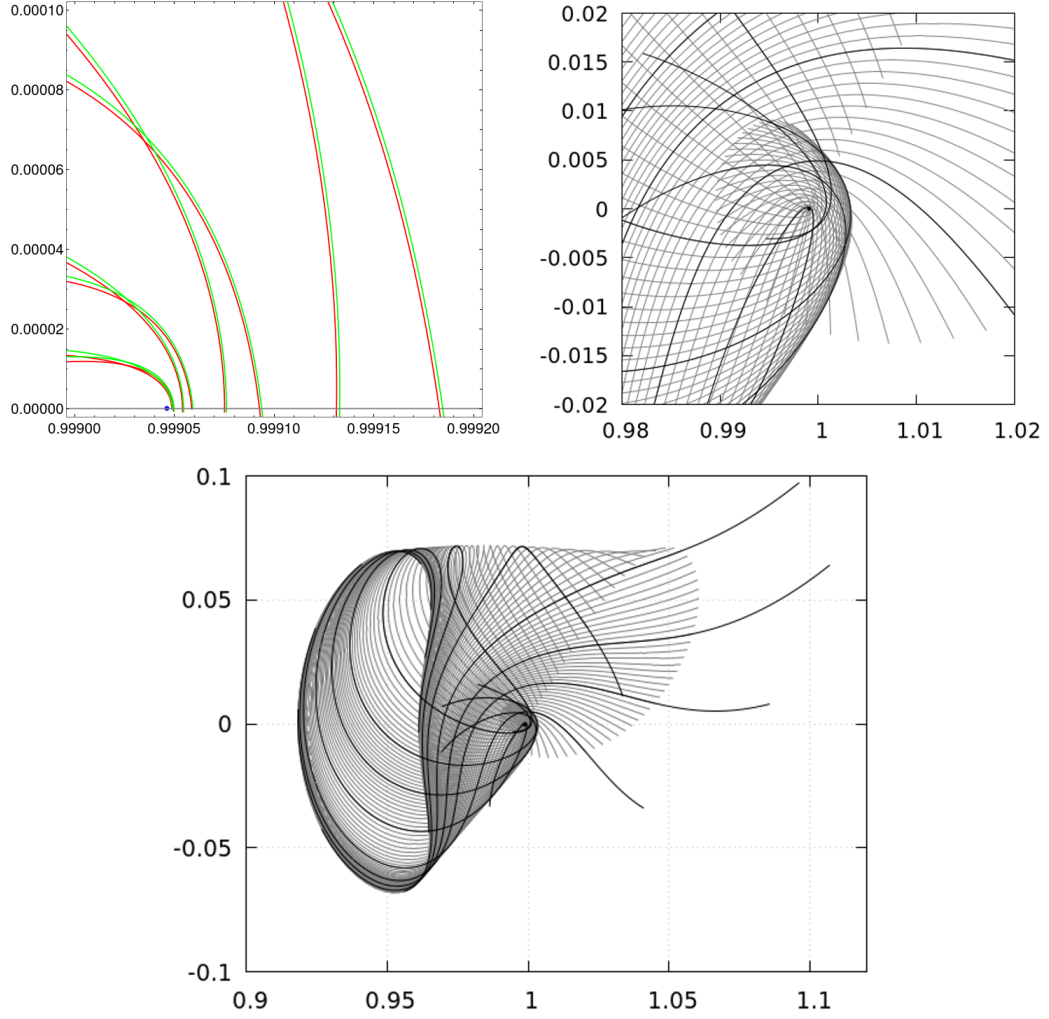


Figure 7: **Top-left panel:** A zoomed in representation of orbits in the inner and outer tube (red and green colors). **Top-right and bottom panels:** Zoomed in representations of orbits in the stable tube for  $a = -0.23$ , already represented in figure 6. The bold black curves represent a selection of orbits which allow to better appreciate the behavior close to the body  $P_2$ .